applied sciences

MDPI

Article

Angioplasty Using 4-Hexylresorcinol-Incorporated Silk Vascular Patch in Rat Carotid Defect Model

Chan-Woo Kim [1], Min-Keun Kim [1], Seong-Gon Kim [1], Young-Wook Park [1], Yong-Tae Park [1], Dae-Won Kim [2] and Hyun Seok [3,*]

1 Department of Oral and Maxillofacial Surgery, College of Dentistry, Gangneung-Wonju National University, Gangneung 25457, Korea; rockerkcw@daum.net (C.-W.K.); omfsmk@gwnu.ac.kr (M.-K.K.); kimsg@gwnu.ac.kr (S.-G.K.); ywpark@gwnu.ac.kr (Y.-W.P.); yudc97@naver.com (Y.-T.P.)

2 Department of Oral Biochemistry, College of Dentistry, Gangneung-Wonju National University, Gangneung 25457, Korea; dwkim@hallym.ac.kr

3 Department of Oral and Maxillofacial Surgery, Chungbuk National University Hospital, Cheongju 28644, Korea

* Correspondence: sok8585@hanmail.net; Tel.: +82-43-269-6387

Received: 2 October 2018; Accepted: 18 November 2018; Published: 26 November 2018



Abstract: The aim of this study was to evaluate and compare the efficacy of 4-hexylresorcinol (4-HR)-incorporated silk as a vascular patch scaffold to that of the commercial polytetrafluoroethylene (PTFE) vascular patch (GORE® ACUSEAL). The expression of the vascular endothelial cell growth factor-A (VEGF-A) after application of 4-HR was studied in RAW264.7 and HUVEC cells. In the animal study, a carotid artery defect was modeled in Sprague Dawley rats (n = 30). The defect was directly closed in the control group (n = 10), or repaired with the PTFE or 4-HR silk patch in the experimental groups (n = 10 per group). Following patch angioplasty, angiography was performed and the peak systolic velocity (PSV) was measured to evaluate the artery patency. The application of 4-HR was shown to increase the expression of VEGF-A in RAW264.7 and HUVEC cells. The successful artery patency rate was 80% for the 4-HR silk group, 30% for the PTFE group, and 60% for the control group. The PSV of the 4-HR silk group was significantly different from that of the control group at one week and three weeks post-angioplasty (p = 0.005 and 0.024). Histological examination revealed new regeneration of the arterial wall, and that the arterial diameter was well maintained in the 4-HR silk group in the absence of an immune reaction. In contrast, an overgrowth of endothelium was observed in the PTFE group. In this study, the 4-HR silk patch was successfully used as a vascular patch, and achieved a higher vessel patency rate and lower PSV than the PTFE patch.

Keywords: silk; 4-hexylresorcinol; vascular patch; angioplasty

1. Introduction

Injury to an artery in the head and neck regions can occur during facial trauma, deformity, cancer, and reconstruction surgeries [1]. For example, branching from the common carotid artery can be damaged during neck dissection, malignant tumor resection, and microvascular free flap transfer in head and neck cancer patients [2]. Although the primary closure method is relatively simple and easy, this technique to repair an arterial defect can increase the risks of postoperative artery aneurysm and restenosis [3]. In contrast, in patch angioplasty, autogenous tissue or an artificial patch material is used to perform artery wall defect closure after the arteriotomy [4]. Patch angioplasty is a common procedure that follows carotid endarterectomy (CEA), which is the removal of the atherosclerotic plaque to reduce the risk of stroke in a patient with internal carotid stenosis [5]. As compared to the primary closure method, patch angioplasty reduces the risks of postoperative stroke, aneurysm, and restenosis [6,7].

Several patch materials were implemented in carotid artery angioplasty, such as autogenous vein, xenogeneic, and synthetic patches [8–10]. The saphenous vein has the advantages of an autogenous tissue surface, a sufficient length for grafting, and a resistance to infection [11]. However, an additional operation is required to harvest the vein, and there is a risk of wound complication at the recipient site [11]. In contrast, the synthetic patch can be made immediately available and does not require any additional surgery for harvesting. In addition, the synthetic patch has a lower risk of postoperative patch rupture and aneurysm dilatation [3]. Commonly used synthetic patch materials include polytetrafluoroethylene (PTFE) and textile Dacron patches [9,12]. Although the synthetic patch has many advantages, it carries a higher risk of infection and foreign-body reaction that can lead to graft failure [13,14]. The ideal non-autogenous patch material should have biocompatibility, allowance for endothelial cell migration, broad availability, and favorable handling [8,15,16]. Although the synthetic patch yielded favorable results in many clinical trials, a more biocompatible and economical biomaterial patch should be developed to reduce the risks associated with artery repair in the oral and maxillofacial region.

Silk derived from the silkworm *Bombyx mori* is a natural biopolymer, and is used as a biomaterial scaffold [17]. Owing to its good biocompatibility and mechanical properties, silk was also used as a suture material for decades [18]. More recently, silk was used in the tissue engineering of scaffolds such as bone, cartilage, artificial tympanic membrane, and vessels [19–21]. A silk cocoon is mainly composed of the two proteins, silk fibroin (SF) and sericin [18]. SF constitutes the core of the silk filament, and is generally used as the post-sericin-removal biomaterial in a process known as degumming [22]. SF has excellent biocompatibility and biodegradability properties, and is used as a vascular tissue scaffold [23]. Furthermore, SF is used as the main component of the small-diameter vascular graft material and vascular patch purposed for vessel repair [23]. However, unlike SF, silk mat derived from cocoons is yet to be employed as a vascular tissue scaffold.

Silk mat can be easily separated from the cocoon to obtain different membrane thicknesses [24]. This separated silk membrane has excellent osteogenic and physical properties, which make it well suited for use as the barrier membrane in guided bone regeneration (GBR) [24,25]. Silk membrane demonstrated good bone regeneration ability in bone defect studies, and has the potential to be employed as a GBR membrane that does not initiate a foreign-body reaction [26]. Silk mat also has mechanical and biological properties that make it well suited for use as a vascular patch material. As an example, silk mat can be processed into thin layers through the process of silk cocoon separation [24]. Additionally, this silk mat demonstrated excellent tensile strength in wet conditions [27]. Considering the qualities of silk mat, we implemented the inner layer of silk mat as a vascular patch scaffold in this study.

The 4-hexylresorcinol (4-HR) natural phenolic compound has antiseptic and antimicrobial activities [28]. This compound was used as a food additive to prevent the melanosis of seafood and fruit, and as antiseptics for skin and oral mucosa [29,30]. It was recently employed as a component in silk-based biomaterials because of its antiseptic and anti-inflammatory activities [31]. In addition, in a microvascular anastomosis study, 4-HR was observed to yield anti-thrombotic effects such as blood coagulation delay and the inhibition of thrombus formation [32]. These effects may be related to its anti-inflammatory activity and the inhibition of transglutaminase-2 (TG-2) activity [33]. When implemented in biomaterials, 4-HR reduces the foreign-body reaction and giant cell formation, and contributes to the biodegradation of the grafted biomaterial [34]. Thus, in this study, 4-HR was used in the fabrication of a silk vascular patch purposed for the prevention of blood coagulation and foreign-body reaction to the silk patch.

Silk can be manufactured into thin layers for application as a vascular-wall biomaterial. We manufactured a silk vascular patch with 4-HR and applied it to correct an artificial vascular defect that is common in angioplasty procedures. We evaluated the efficacy of the 4-HR-incorporated silk as a vascular patch in a rat carotid defect model and compared it to that of the commercial product.

2. Materials and Methods

2.1. Cellular Experiment

RAW264.7 cells (Korean Cell Line Bank No. 40071) and HUVEC cells (ATCC, Manassas, VA, USA) were used for this experiment. Cultured cells were placed in six-well plates and administered 4-HR in concentrations of 1, 5, or 10 μg/mL (Sigma-Aldrich, St. Louis, MO, USA). Complete proteins from cells were collected at 2, 8, and 24 h after administration and subsequently mixed into a buffer solution and denatured through the application of heat. Then, the proteins were electrophoresed and the gels were transferred to membranes. Following the blocking procedure, diluted vascular endothelial growth factor-A (VEGF-A) primary antibody (Santa Cruz Biotech, Santa Cruz, CA, USA) was applied. For comparative purposes, β-actin from Sigma-Aldrich was used as an internal control. The blots were imaged using the ChemiDoc XRS system (Bio-Rad Laboratories, Hercules, CA, USA).

2.2. Blood Coagulation Test

Firstly, 0.1 M 4-HR was solubilized into 1 L of normal saline until saturation, and the supernatant was collected. Then, 100 μL of the supernatant was mixed with 1000 μL of normal saline. The final concentration of 4-HR in the normal saline was 9 mM. Whole blood was collected from New Zealand white rabbits (Samtako Biokorea, Osan, Korea). For the experimental group, 40 μL of 4-HR solution was added to 500 μL of blood. For the control group, the same volume of normal saline was added to blood. Then, the absorbance was measured by using a spectrometer (Optizen 3220UV, Daejeon, Korea), with a higher value corresponding to increased coagulation.

2.3. Experimental Animals

A total of 30 12-week-old Sprague Dawley rats (Samtako Biokorea, Osan, Korea) with an average weight of 250 g (range 200–300 g) were used in this study. The rats were individually caged under specific pathogen-free conditions and provided a standard rodent diet and water ad libitum. The animals were acclimated for 10 days before the surgery. This study was approved by the Institutional Animal Care and Use Committee of Gangneung-Wonju National University, Gangneung, Korea (GWNU-2013-32).

2.4. Patch Materials and Scanning Electron Microscopy (SEM) Examination

2.4.1. Preparation of 4-HR-Incorporated Silk Patch

Silk cocoon derived from the silkworm *Bombyx mori* was supplied by the Rural Development Administration (Jeonju, Korea) for medical application. The peeling method was used to separate natural silk cocoon into layers of varying thickness [24]. The silk patch was manufactured using microsurgical instruments (S&T, Neuhausen, Switzerland) to peel away the cocoon under a microscope (OPMI MD S5, Zeiss, Germany). The desired thickness of the innermost silk layer was carefully peeled off and used as the silk patch. The 4-HR was dissolved in ethyl alcohol to prepare a 3% 4-HR solution. The silk patch was then placed into the 3% 4-HR solution for 24 h before being dried in an oven at 45 °C. Following vaporization of the ethyl alcohol, the 4-HR silk patch was sterilized with ethylene oxide gas and prepared at room temperature.

2.4.2. PTFE Patch

The PTFE patch was used in a patch angioplasty procedure for cardiovascular reconstruction. ACUSEAL patches (GORE® ACUSEAL Cardiovascular Patch, Flagstaff, AZ, USA) were purchased and used in this study as the commercial patch. The SEM images of the 4-HR silk and PTFE patches were examined using an electron microscope (SU-70; Hitachi, Japan) operating at 5 keV.

2.5. Study Design and Surgical Procedure

Thirty rats were randomly divided into three groups and anesthetized via intramuscular injection of a combination of Zoletil 50 (15 mg/kg; Vibac, Carros, France) and Rumpun (0.2 mL/kg; Bayer Korea, Seoul, Korea). The ventral cervical region was shaved and disinfected with povidone-iodine before surgery. A 2% lidocaine with epinephrine (1:100,000) mixture was administrated in the cervical region for local anesthesia. A midline cervical incision was made, and the dissection was performed under a microscope (OPMI MD S5, Zeiss, Germany) using sterile microsurgical instruments (S&T, Neuhausen, Switzerland). The superficial dissection originated at the cervical muscle and extended downward to the carotid artery. After achieving adequate exposure of the right carotid artery, the proximal and distal ends of the artery were secured with a microvascular clamp. A rectangular-shaped full-thickness defect (0.5 mm $\times$ 1 mm) was made by excising the arterial wall using micro-scissors. In the control group (n = 10), the defect was directly closed with 10-0 monofilament nylon (Ailee Co., Ltd., Busan, Korea). The PTFE and 4-HR silk patches were respectively employed in the patch angioplasty procedures performed on the animals in the experimental groups. In both groups, the patch size was 2 mm $\times$ 2 mm. In the PTFE group (n = 10), the square PTFE patch covered the arterial defect, and each side of the patch was sutured to the arterial wall with 10-0 nylon. The same procedure was used to apply the 4-HR silk patch to cover the arterial defect in the 4-HR silk group (n = 10). The empty and refill test was subsequently used to confirm vessel patency in all groups [35]. The wire was tagged at the proximal and distal ends of the artery in order to enable detection, and arterial patency was monitored using ultrasonography and angiography. The superficial muscle and skin were closed with 3-0 vicryl (VICRYL®, Ethicon, USA) and black silk (AILEE, Busan, Korea). Gentamycin (1 mg/kg; Kookje, Seoul, Korea) and pyrin (0.5 mL/kg; Green Cross Veterinary Products, Seoul, Korea) were intramuscularly injected into the animals three times per day over a period of three days.

2.6. Ultrasonography and Angiography

After performing patch angioplasty, ultrasonography was used to assess the carotid artery in order to evaluate its arterial patency. An ultrasound system (ACCUVIX V10®, Samsung medison, Seongnam, Korea) was used to perform ultrasonography on anesthetized animals immediately after the operation, and at one week and three weeks post-operation. The carotid artery between the tagged wire was detected during Doppler ultrasonography, and the peak systolic velocity (PSV) was measured.

The angiogram was taken three weeks after the operation. After exposing a branch of the inferior vena cava, 3 mg of the contrast media (VISPAQUE®, GE healthcare, Marlborough, MA, USA) was injected. Then, radiography was performed on the neck area.

2.7. Histological Analysis

All artery samples were harvested three weeks after the angioplasty procedure. Prior to sample harvesting, to maintain the arterial diameter, both ends of the artery were ligated with nylon after it was filled with blood. The samples were fixed in 10% formalin, and dehydrated in ethyl alcohol and xylene. The samples were cross-sectioned in the area of the patch angioplasty and embedded into paraffin blocks, which were subsequently sliced into sections and stained with hematoxylin and eosin. The resulting sections showed the cross-sectional view and diameter of the artery. Digital images of the selected sections were obtained using a digital camera (DP-73; Olympus, Tokyo, Japan).

2.8. Fluorescent and Immunohistochemical Analysis of Endothelial Cell Marker

The paraffin sections were subjected to deparaffinization and hydration before H_2O_2 was applied to block endogenous peroxidase activity; a serum-free blocking agent was used to achieve blocking. The primary antibody for von Willebrand factor (vWF; CAT#: sc-365712, Santa Cruz Biotechnology, Santa Cruz, CA, USA) was applied as 1:100 dilutions and incubated overnight at 4 °C. After washing the sections with phosphate-buffered saline (PBS), fluorescein isothiocyanate (FITC)-conjugated

secondary antibody (1:1000 dilutions) was applied, and the sections were counterstained with 4′,6-diamidino-2-phenylindole (DAPI).

Immunohistochemistry (IHC) was performed on the histological sections to evaluate the expression of vWF; anti-vWF was used as the primary antibody. Immunohistochemical staining was performed by using a Dako REAL EnVision Detection System (Dako, Glostrup, Denmark) according to the manufacturer's protocols, and Mayer's hematoxylin (Sigma-Aldrich) was used as the counterstain. The stained tissue slides were examined using an Olympus BX51 (Olympus, Tokyo, Japan) microscope.

2.9. Statistical Analysis

The chi-square method was applied to compare the arterial patency between groups, and one-way analysis of variance (ANOVA) was used to compare the PSV. Additionally, the least significance difference test was utilized for post hoc analysis. Differences with p-values of less than 0.05 were considered significant.

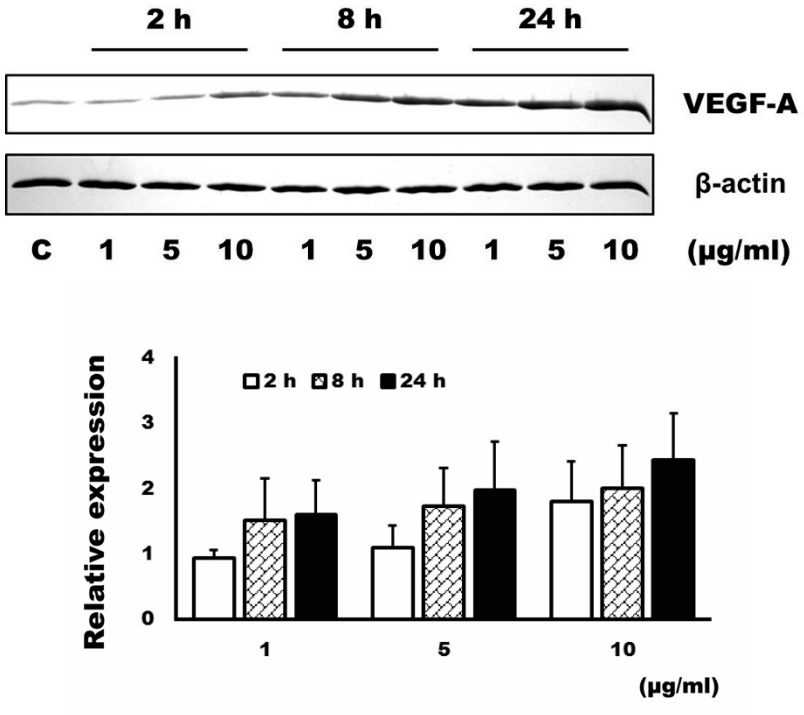
3. Results

3.1. Expression Level of VEGF-A after Administration of 4-HR

The administration of 4-HR increased the expression level of VEGF-A in HUVEC cells (Figure 1). As can be seen, the expression level of VEGF-A was dependent on the dose and time of the 4-HR application.

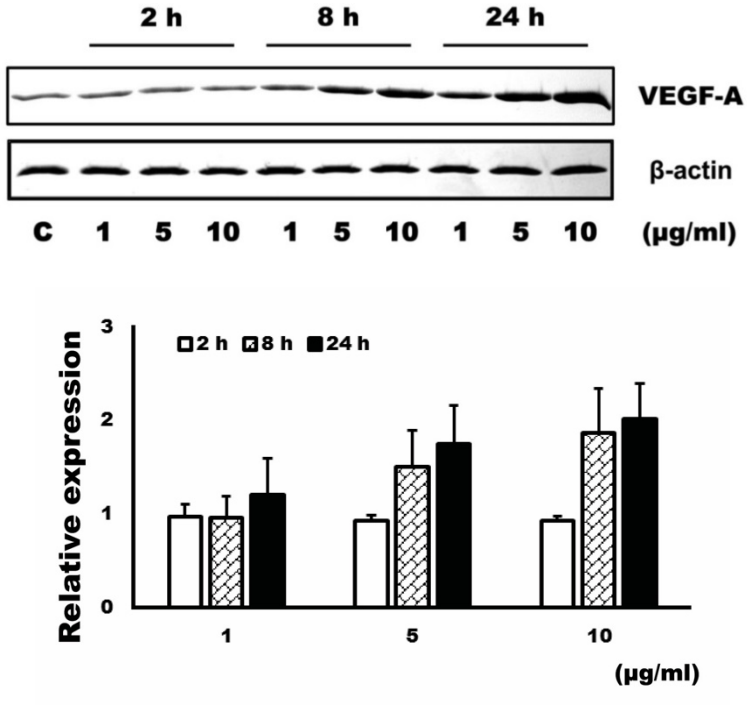
3.2. Blood Coagulation Test

The absorbance of the 4-HR was 1.21 ± 0.13 nm, and that of the control was 1.53 ± 0.13 nm. The difference between groups was statistically significant (p = 0.034).



(**a**)

Figure 1. *Cont.*



(**b**)

Figure 1. Western blot analysis for 4-hexylresorcinol (4-HR). The application of 4-HR increased the expression level of vascular endothelial growth factor-A (VEGF-A) in (**a**) RAW264.7, and (**b**) HUVEC cells (C: untreated control).

3.3. SEM Morphology Results for the 4-HR Silk and PTFE Patches

SEM images of the 4-HR silk and PTFE patches are presented in Figure 2. Cross-linking of the silk fiber can be observed in the 4-HR silk patch image. This structure provided a level of porosity that enabled migration of the regenerative endothelial cells. The diameter of the silk fiber was approximately 100 μm (Figure 3a). Conversely, although the surface of the PTFE patch largely appeared to be smooth, part of the surface appeared to be torn (Figure 3b).

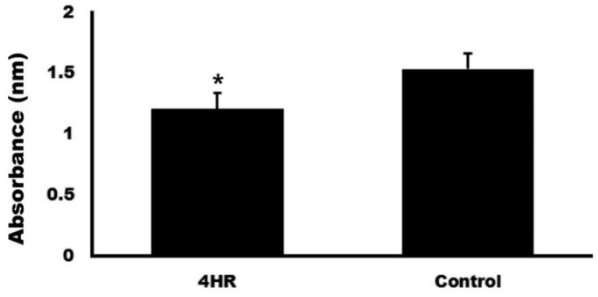
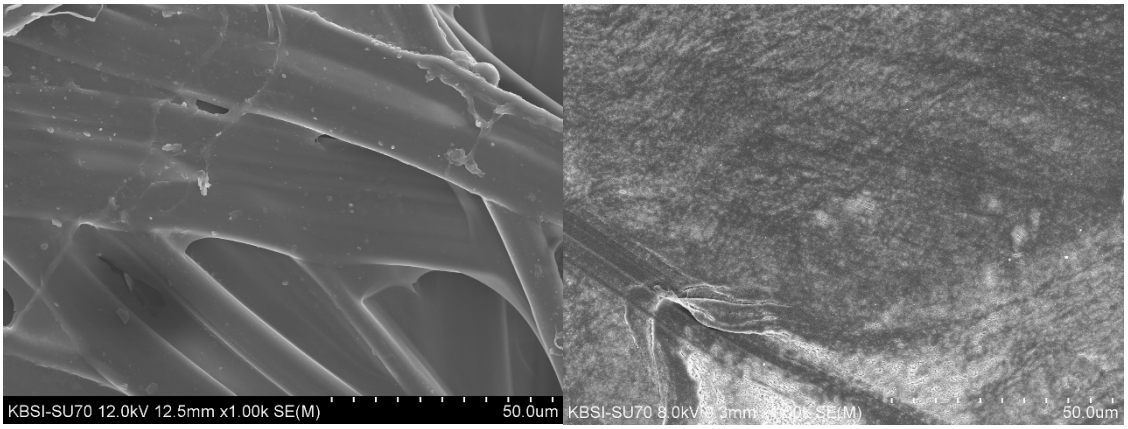


Figure 2. Blood coagulation test results. The absorbance of the 4-HR was significantly different from that of the control (p = 0.034).

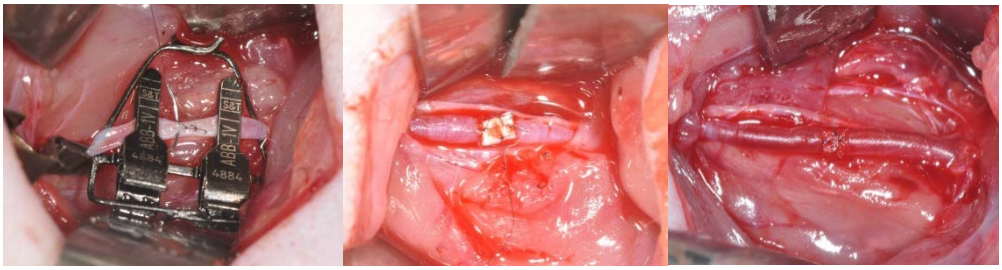
3.4. Artery Patency after Patch Angioplasty

Gross artery patency was confirmed via the empty and refill test, and an acceptable degree of patency was observed in all groups during the operation (Figure 4). In the PTFE group, blood leakage was observed around the patch-covered area, and a sufficient amount of time was required to confirm hemostasis (Figure 4b). Less blood leakage and good adhesion to the covered arterial tissue and wall were observed in the 4-HR silk patch group (Figure 4c).



(**a**) (**b**)

Figure 3. SEM images of patch materials: (**a**) 4-HR-incorporated silk patch and; (**b**) polytetrafluoroethylene (PTFE) patch.

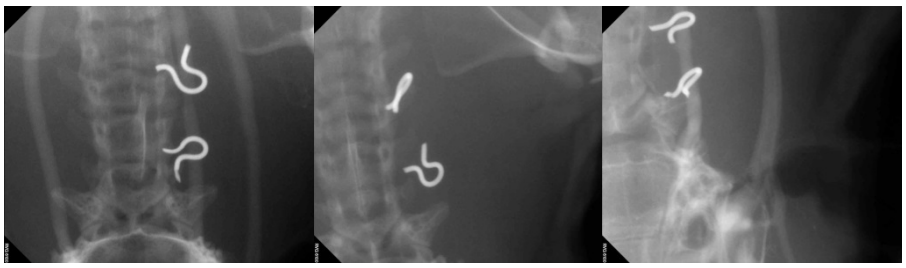


(**a**) (**b**) (**c**)

Figure 4. Repair of the artificial carotid artery defect: (**a**) direct closure of the artery defect as control group; patch angioplasty with (**b**) PTFE patch, and (**c**) 4-HR silk patch.

The artery patency of each group is presented in Figure 4. Successful artery patency was observed in eight rats in the 4-HR silk group (80%), as compared to only three rats (30%) in the PTFE group. The direct closure group showed success in six rats (60%). There was a statistically significant difference between the 4-HR silk group and PTFE group ($p = 0.035$). However, there was no significant difference between any other group ($p > 0.05$).

The results of angiography are shown in Figure 5. Narrowing of the carotid artery was observed at the repaired site in the direct closure group (Figure 5a). In the PTFE group, loss of vascular patency was manifested as a signal void between the wire tags (Figure 5b). The arterial diameter of the animals in the 4-HR silk group did not change after patch angioplasty, and was stably maintained better than that on the contralateral side of the carotid artery (Figure 5c).



(**a**) (**b**) (**c**)

Figure 5. Three-week post-operation angiography: (**a**) direct closure as the control group; (**b**) PTFE patch angioplasty; (**c**) 4-HR silk patch angioplasty.

3.5. Ultrasonography PSV Results

At one week post-angioplasty, the PSV for the 4-HR silk group was 41.20 ± 7.92 cm/s, and those of the PTFE and control groups were 32.74 ± 10.50 cm/s and 75.23 ± 27.05 cm/s, respectively (Figure 6). There was a statistically significant difference among all groups (p = 0.007). Furthermore, in the post hoc test, the PSVs for the 4-HR silk and PFTE groups were both significantly different from that of the control group (p = 0.005). The three-week post-angioplasty PSV results for the 4-HR silk, PTFE, and control groups were 35.92 ± 1.45 cm/s, 35.36 ± 7.27 cm/s, and 48.36 ± 6.15 cm/s, respectively (Figure 6); there was a statistically significant difference among all groups (p = 0.029). In the post hoc test, the PSVs for the 4-HR silk group and PFTE group were significantly different from that of the control group, with p = 0.024 and p = 0.020, respectively.

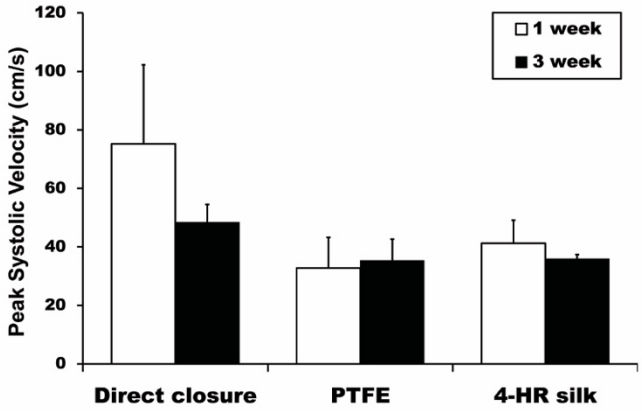
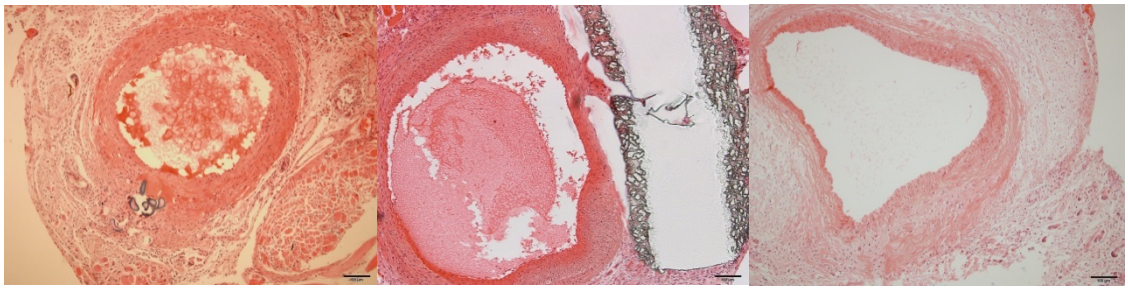


Figure 6. One-week and three-week post-angioplasty peak systolic velocity (PSV) results for all three groups. One-week post-operation results yielded a statistically significant difference among all groups (p = 0.007). The PSVs for the 4-HR silk and PTFE groups were significantly different than that for the control group (p = 0.005). Three-week post-operation results yielded a statistically significant difference among all groups (p = 0.029). The control group PSV result was significantly different from that of the PTFE and 4-HR silk groups, with p = 0.020 and 0.024, respectively.

3.6. Histological Examination

Low inflammation and foreign-body reaction around the patch material were observed in the 4-HR silk group (Figure 7). Regeneration of the arterial wall in the defect was also observed, and the diameter and shape of the artery were found to be well maintained. Although the shape and diameter of the artery was well maintained in the PTFE group, overgrowth of the arterial wall was observed in several artery samples (Figure 7). It should also be noted that the control group had the overall smallest arterial diameter, and the arterial wall tended to collapse more than any other group (Figure 7).



(**a**) (**b**) (**c**)

Figure 7. Three-week post-operation histological examination results: (**a**) direct closure as the control group; (**b**) PTFE group; (**c**) 4-HR silk group (hematoxylin and eosin stain, original magnification ×100, scale bar = 100 μm).

3.7. Fluorescent and Immunohistochemical Examination of vWF Expression

The 4-HR silk group showed a higher level of vWF expression in the endothelial layer (Figure 8). As can be seen in Figure 8, remnants of the silk patch demonstrated a mild level of fluorescence (S), and the size of the vascular lumen (L) was maintained. In the case of the direct closure control group, a high level of vWF expression was observed in the vascular lumen. However, the size of the vascular lumen (L) was smaller than that of the 4-HR silk group. Additionally, the vascular lumen (L) of the PTFE group tended to be relatively very small, and intimal hyperplasia and a low level of vWF expression were evident in the PTFE group.

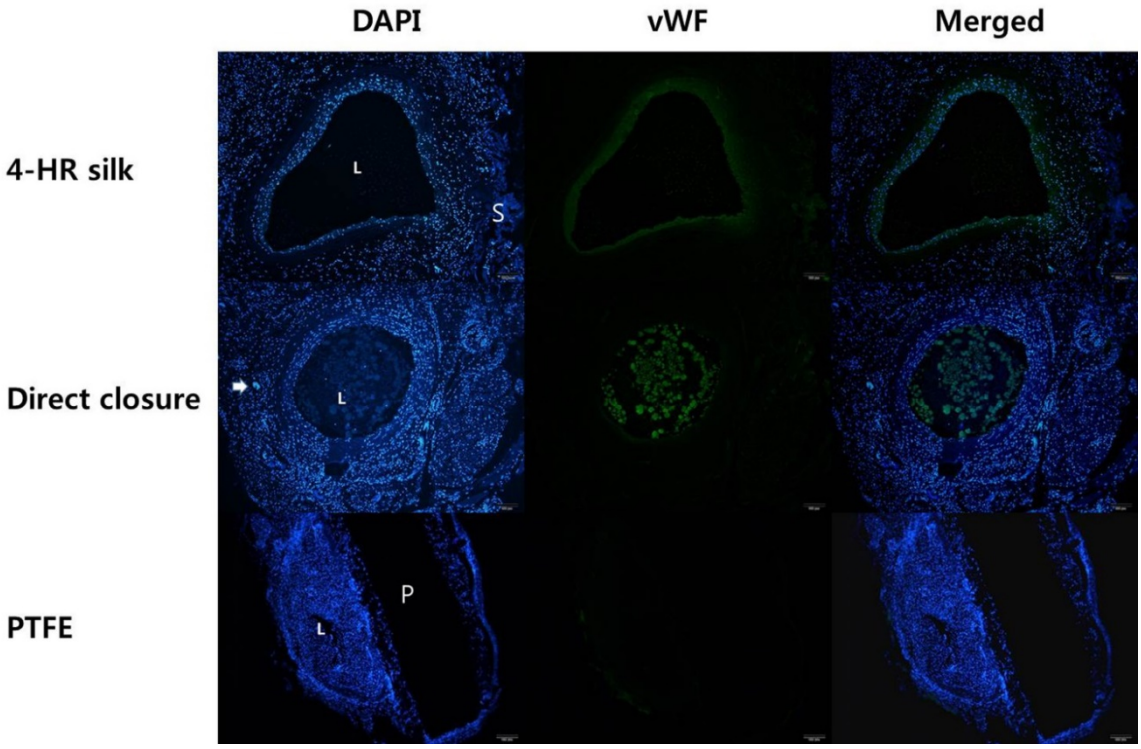


Figure 8. Fluorescence examination results for von Willebrand factor (vWF) expression (L: lumen, S: silk patch; original magnification ×100, scale bar = 100 μm).

The vWF expression levels of the animals in the 4-HR silk group were evaluated three weeks after the angioplasty operation (Figure 9). The results revealed a high level of vWF expression in the regenerated endothelium of the 4-HR silk group.

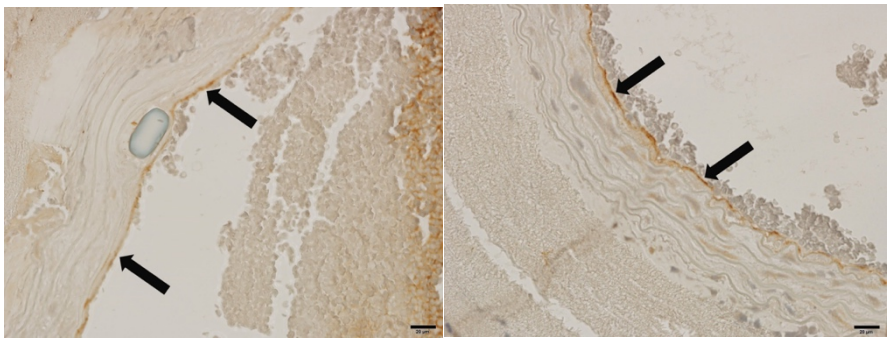


Figure 9. The 4-HR silk group vWF expression immunohistochemical results (Original magnification ×500, scale bar = 20 μm). The black arrows indicate vWF-positive areas.

4. Discussion

Silk derived from silkworms was used in various tissue engineering fields as a natural biopolymer scaffold [26,36] owing to its excellent biological properties, such as biocompatibility, biodegradability, and tissue affinity [37]. Other reasons for choosing to employ silk as a vascular tissue engineering scaffolding biomaterial are its low thrombotic and immunologic properties and ease of clinical handling [37,38]. In consideration of these properties, silk was processed into various forms of vascular scaffolds, such as tubes, films, and patches [39–41]. Specifically, studies that employed SF as an artificial vessel confirmed it to have excellent hemocompatibility, cell viability, tissue integrity, and mechanical strength [42–44]. SF was also incorporated into cardiovascular patches purposed for vascular surgery [41,45]. Additionally, an in vivo study confirmed SF to have favorable biological and physical properties, and that it can be effectively used in vessel reconstruction surgery [41].

Silk mat from silk cocoons has various biological and mechanical properties that make it suitable for use as a vascular patch [24]. As an example, silk mat can be easily and economically manufactured by merely peeling the silk cocoon [24], thus making its manufacturing process simpler than that of the SF vascular patch [40]. Furthermore, vascular patch material should have enough mechanical strength to resist suture retention [41]. Thus, in a previous study, silk mat was evaluated as a patch material against collagen and PTFE membranes; the results revealed silk mat to have the highest tensile strength under wet conditions [27]. In addition, silk mat was demonstrated to have excellent suture-retention strength as compared to collagen [24]. In our study, a 4-HR-incorporated silk patch was manufactured by peeling a silk cocoon. This 4-HR silk patch was applied to a carotid artery defect by suturing it to the arterial wall; consequently, no tearing was observed under the wet conditions (Figure 4c).

Silk derived from silkworms consists of fibroin and sericin [17]. Fibroin constitutes the core of the silk filament [46], while sericin is attached to the fibroin fibers and acts to bind them together [47]. During patch angioplasty, there was no excessive blood leakage in any group, and artery patency was confirmed via angiography (Figures 4 and 5). However, some blood leakage was observed around the patch in the PTFE group after the operation (Figures 4 and 5). As compared to the PTFE patch group, the 4-HR silk patch group had less blood leakage and good adhesion to the arterial wall (Figure 4b). As sericin is a bonding protein [47], it may have enhanced the attachment of the silk patch to the vessel.

Patch angioplasty was reported to reduce the risk of stroke and restenosis more effectively than the primary closure method in a carotid stenosis patient [8]. This is likely due to the fact that primary closure of the small-diameter carotid artery following endarterectomy affects the blood flow in the narrow artery, and can increase the risk of postoperative restenosis [48,49]. In our study, the angiography results showed that, in the control group, the diameter of the artery was substantially reduced after direct closure. In contrast, the arterial diameter of the animals in the 4-HR silk and PTFE groups tended to be stably maintained, with no significant reduction. Additionally, an acceptable rate of blood flow was observed in the 4-HR silk and PTFE groups using ultrasonography (Figure 6). The PSV of the 4-HR silk group significantly differed from that of the control group at one week and three weeks after the angioplasty operation ($p = 0.005$ and 0.024, respectively). Significant differences between the one- and three-week PSVs of the PTFE group and those of the control group were also determined ($p = 0.005$ and 0.020, respectively). Furthermore, according to the ultrasonography results, the velocity of blood flow in the control group significantly differed from that observed in the other groups ($p < 0.05$). This indicates that the diameter of artery was reduced, and that this reduction increased the blood flow velocity in the direct closure area. According to the results of the angiography, the blood flow velocities of the 4-HR silk and PTFE groups did not change after the angioplasty operation. This finding confirmed that the patch angioplasty can repair an arterial wall defect more effectively than the direct closure method. Furthermore, the efficacy of the 4-HR silk patch as a patch material was found to be comparable to that of the commercial PTFE patch product.

Autogenous veins and xenogeneic and synthetic materials are used as vascular patch materials [50]. As a synthetic patch material, PTFE demonstrated acceptable suture strength and mechanical strength through its ability to resist blood pressure increase [51]. However, it carries the risk of inducing a

foreign-body response that leads to chronic inflammation and thrombus formation [52]. The implanted synthetic biomaterial functions as a foreign body to the host, and control of this immune reaction is key to the success of the graft [53]. Foreign-body reaction and giant cell formation often occur around the implanted material, and can lead to graft failure and retrieval [53,54]. Furthermore, although the PTFE material was successfully employed as a vascular patch in clinical applications, rare cases of infection and pseudoaneurysm after angioplasty were reported [9,14]. In our experiment, severe aneurysm and granuloma formation were observed in the PTFE group. In contrast, in the 4-HR silk group, no signs of restenosis or an aneurysm were observed, and there was stable blood flow. Moreover, as previously reported, the 4-HR-incorporated silk cocoon demonstrated excellent biocompatibility as a vascular patch scaffold, and did not induce any severe immunological reaction [26].

The 4-HR compound has anti-microbial activity and is used as an antiseptic [55]. In consideration of these characteristics, in this study, 4-HR was used as a material component in the silk patch in order to prevent bacterial infection and an immune reaction, as this compound is known to inhibit foreign-body reaction and giant cell formation around the graft material area [31]. The 4-HR compound inhibits foreign-body giant cell formation via suppression of the diacylglycerol kinase in macrophages, and induces the biodegradation of the graft material [31,34]. Thus, 4-HR is associated with soft-tissue healing and regeneration [56]. Furthermore, it inhibits tumor necrosis factor-α (TNF-α) expression in raw cells, and contributes to the rapid epithelization and collagen regeneration in burn wounds [56]. In our histological examination, we did not observe any inflammatory or immunological reaction in the 4-HR silk group. Instead, a newly regenerated endothelium was observed near the silk patch (Figure 7). The fluorescence and immunohistochemical examination results for the 4-HR silk group revealed a high level of vWF expression in the regenerated endothelium, and a well-maintained vascular lumen (Figures 8 and 9). In summary, 4-HR was not only demonstrated to be effective, but it was found to contribute to the success of the silk patch angioplasty by reducing the immune reaction and inducing endothelium regeneration.

In a recent study, the proteins released from the silk mat of the silkworm cocoon were associated with an angiogenesis effect [57]. As previously mentioned, silk mat from the cocoon can be divided into layers of varying thickness by peeling the inner and outer layers [24]. Proteins released from the inner layer of the silk mat can induce expression of the angiogenesis-related gene [57]. In particular, the Wingless-type Murine mammary tumor virus (MMTV) integration site family, member 3A (Wnt3a) protein is associated with macrophage-mediated angiogenesis, and is overexpressed by the protein solution from the inner silk layer [58]. Moreover, the platelet-derived growth factor gene, which plays a significant role in angiogenesis, is also overexpressed in the protein solution from the inner silk layer [57]. These factors are believed to have contributed to the increased expression level of VEGF-A, which plays a critical role in angiogenesis, that was observed in the 4-HR silk patch group (Figure 1) [59].

In in vitro studies, 4-HR demonstrated anti-thrombotic effects in microvascular anastomosis by delaying blood coagulation and inhibiting thrombus formation in vascular anastomosis [32]. Additionally, venous thrombosis is critical to the success of microvascular free-flap transfer and angioplasty [60,61]. In our study, incorporating 4-HR was found to induce anti-thrombotic effects in the blood coagulation test (Figure 2). This result confirmed that incorporating 4-HR as a material component of the silk patch contributes to the prevention of thrombosis in the vessel after patch angioplasty. Moreover, new regeneration of the arterial wall was observed in the artificial defect, and the diameter of artery was well maintained in the absence of any inflammatory reaction (Figures 8 and 9). In contrast, although the arterial diameter was generally well maintained, some endothelial overgrowth was observed in the PTFE group (Figure 7). Furthermore, in the control group, the artery tended to be narrowed and severely shrunken in the direct closure area; this phenomenon caused the non-angioplasty control group to have the highest blood flow velocity. These results indicated that patch angioplasty can effectively repair small-diameter artery defects, as it was demonstrated to provide good arterial patency and blood flow as compared to results of the direct closure method.

Thus, we demonstrated that the 4-HR silk patch can be effectively used as a patch material, and that it has higher biocompatibility and hemocompatibility than the PTFE patch.

5. Conclusions

In this study, we used 4-HR-incorporated silk mat as a vascular patch purposed to repair an artery defect in a rat carotid defect model. The silk patch has significant advantages as a patch scaffold, such as high biocompatibility, sufficient mechanical strength to resist suture retention even in wet conditions, and easy clinical handling for micro-suturing. Furthermore, the silk patch is an economical and easily processed biomaterial for use as a patch scaffold. In this study, 4-HR was used as a material component of the silk vascular patch, as it inhibits any foreign-body reaction to the graft material. In addition, 4-HR was demonstrated to possess anti-thrombotic characteristics and induce soft-tissue healing by inhibiting the expression of the inflammatory cytokine proteins. The properties of 4-HR were confirmed to contribute to immune reaction suppression and thrombus formation prevention, and induce endothelium healing in patch angioplasty. Thus, in conclusion, the 4-HR silk patch was effectively employed as a carotid artery defect patch scaffold, and the results confirmed that it has efficacy that is comparable to that of a commercially available vascular patch. However, although the 4-HR silk patch was successfully implemented in patch angioplasty, further study is needed to evaluate its long-term biological and mechanical stability as a patch material prior to clinical application.

Author Contributions: S.-G.K. and M.-K.K. conceived and designed the experiments; C.-W.K., D.-W.K., and M.-K.K. performed the experiments; C.-W.K., M.-K.K., and S.-G.K. analyzed the data; H.S. wrote the first draft, and Y.-W.P. and S.-G.K. reviewed and edited the paper. All of the authors read and approved the final version of the manuscript.

Funding: This research received no external funding.

Acknowledgments: This work was carried out with the support of "Cooperative Research Program for Agriculture Science and Technology Development (Project No. PJ01313902)", Rural Development Administration, Republic of Korea.

Conflicts of Interest: The authors declare no conflict of interest.

References

1. Ketcham, A.S.; Hoye, R.C. Spontaneous carotid artery hemorrhage after head and neck surgery. *Am. J. Surg.* **1965**, *110*, 649–655. [CrossRef]
2. Powitzky, R.; Vasan, N.; Krempl, G.; Medina, J. Carotid blowout in patients with head and neck cancer. *Ann. Otol. Rhinol. Laryngol.* **2010**, *119*, 476–484. [CrossRef] [PubMed]
3. Kim, J.H.; Cho, Y.P.; Kwon, T.W.; Kim, H.; Kim, G.E. Ten-year comparative analysis of bovine pericardium and autogenous vein for patch angioplasty in patients undergoing carotid endarterectomy. *Ann. Vasc. Surg.* **2012**, *26*, 353–358. [CrossRef] [PubMed]
4. Papakostas, J.C.; Avgos, S.; Arnaoutoglou, E.; Nassis, C.; Peroulis, M.; Bali, C.; Papadopoulos, G.; Matsagkas, M.I. Use of the vascu-guard bovine pericardium patch for arteriotomy closure in carotid endarterectomy. Early and long-term results. *Ann. Vasc. Surg.* **2014**, *28*, 1213–1218. [CrossRef] [PubMed]
5. Walker, M.D.; Marler, J.R.; Goldstein, M.; Grady, P.A.; Toole, J.F.; Baker, W.H.; Castaldo, J.E.; Chambless, L.E.; Moore, W.S.; Robertson, J.T. Endarterectomy for asymptomatic carotid artery stenosis. *JAMA* **1995**, *273*, 1421–1428. [CrossRef]
6. AbuRahma, A.F.; Robinson, P.A.; Saiedy, S.; Khan, J.H.; Boland, J.P. Prospective randomized trial of carotid endarterectomy with primary closure and patch angioplasty with saphenous vein, jugular vein, and polytetrafluoroethylene: Long-term follow-up. *J. Vasc. Surg.* **1998**, *27*, 222–234. [CrossRef]
7. AbuRahma, A.F.; Stone, P.; Deem, S.; Dean, L.S.; Keiffer, T.; Deem, E. Proposed duplex velocity criteria for carotid restenosis following carotid endarterectomy with patch closure. *J. Vasc. Surg.* **2009**, *50*, 286–291. [CrossRef] [PubMed]
8. Bond, R.; Rerkasem, K.; Naylor, A.; Aburahma, A.; Rothwell, P. Systematic review of randomized controlled trials of patch angioplasty versus primary closure and different types of patch materials during carotid endarterectomy. *J. Vasc. Surg.* **2004**, *40*, 1126–1135. [CrossRef] [PubMed]

9. Stone, P.A.; Srivastava, M.; Campbell, J.E.; Mousa, A.Y.; Hass, S.H.; Kazmi, H.; Dearing, D.D.; AbuRahma, A.F. A 10-year experience of infection following carotid endarterectomy with patch angioplasty. *J. Vasc. Surg.* **2011**, *53*, 1473–1477. [CrossRef] [PubMed]
10. Oldenburg, W.A.; Almerey, T.; Selim, M.; Farres, H.; Hakaim, A.G. Durability of carotid endarterectomy with bovine pericardial patch. *Ann. Vasc. Surg.* **2018**, *50*, 218–224. [CrossRef] [PubMed]
11. Kamenskiy, A.V.; MacTaggart, J.N.; Pipinos, I.I.; Gupta, P.K.; Dzenis, Y.A. Hemodynamically motivated choice of patch angioplasty for the performance of carotid endarterectomy. *Ann. Biomed. Eng.* **2013**, *41*, 263–278. [CrossRef] [PubMed]
12. Chou, D.; Tulloch, A.; Cossman, D.V.; Cohen, J.L.; Rao, R.; Barmparas, G.; Mirocha, J.; Wagner, W. The influence of collagen impregnation of a knitted dacron patch used in carotid endarterectomy. *Ann. Vasc. Surg.* **2017**, *39*, 209–215. [CrossRef] [PubMed]
13. Awad, I.A.; Little, J.R. Patch angioplasty in carotid endarterectomy. Advantages, concerns, and controversies. *Stroke* **1989**, *20*, 417–422. [CrossRef] [PubMed]
14. Terzian, W.H.; Schadt, S.; Sheth, S.U. Right carotid-cutaneous fistula and right carotid pseudoaneurysm formation secondary to a chronically infected polyethylene terephthalate patch. *Int. J. Crit. Illn. Inj. Sci.* **2018**, *8*, 48–51. [CrossRef] [PubMed]
15. Ratcliffe, A. Tissue engineering of vascular grafts. *Matrix Biol.* **2000**, *19*, 353–357. [CrossRef]
16. Zhang, W.J.; Liu, W.; Cui, L.; Cao, Y. Tissue engineering of blood vessel. *J. Cell. Mol. Med.* **2007**, *11*, 945–957. [CrossRef] [PubMed]
17. Cao, Y.; Wang, B. Biodegradation of silk biomaterials. *Int. J. Mol. Sci.* **2009**, *10*, 1514–1524. [CrossRef] [PubMed]
18. Aigner, T.B.; DeSimone, E.; Scheibel, T. Biomedical applications of recombinant silk-based materials. *Adv. Mater.* **2018**, *30*, 1704636. [CrossRef] [PubMed]
19. Ghassemifar, R.; Redmond, S.; Zainuddin; Chirila, T.V. Advancing towards a tissue-engineered tympanic membrane: Silk fibroin as a substratum for growing human eardrum keratinocytes. *J. Biomater. Appl.* **2010**, *24*, 591–606. [CrossRef] [PubMed]
20. Jo, Y.Y.; Kim, S.G.; Kwon, K.J.; Kweon, H.; Chae, W.S.; Yang, W.G.; Lee, E.Y.; Seok, H. Silk fibroin-alginate-hydroxyapatite composite particles in bone tissue engineering applications in vivo. *Int. J. Mol. Sci.* **2017**, *18*, 858. [CrossRef] [PubMed]
21. Park, Y.T.; Kwon, K.J.; Park, Y.W.; Kim, S.G.; Kim, C.W.; Jo, Y.Y.; Kweon, H.Y.; Kang, S.W. The effect of silk fibroin/nano-hydroxyapatite/corn starch composite porous scaffold on bone regeneration in the rabbit calvarial defect model. *Maxillofac. Plast. Reconstr. Surg.* **2011**, *33*, 459–466.
22. Khan, M.M.R.; Tsukada, M.; Gotoh, Y.; Morikawa, H.; Freddi, G.; Shiozaki, H. Physical properties and dyeability of silk fibers degummed with citric acid. *Bioresour. Technol.* **2010**, *101*, 8439–8445. [CrossRef] [PubMed]
23. Lovett, M.; Cannizzaro, C.; Daheron, L.; Messmer, B.; Vunjak-Novakovic, G.; Kaplan, D.L. Silk fibroin microtubes for blood vessel engineering. *Biomaterials* **2007**, *28*, 5271–5279. [CrossRef] [PubMed]
24. Kweon, H.; Jo, Y.Y.; Seok, H.; Kim, S.G.; Chae, W.S.; Sapru, S.; Kundu, S.C.; Kim, D.W.; Park, N.R.; Che, X. In vivo bone regeneration ability of different layers of natural silk cocoon processed using an eco-friendly method. *Macromol. Res.* **2017**, *25*, 806–816. [CrossRef]
25. Yoo, C.K.; Jeon, J.Y.; Kim, Y.J.; Kim, S.G.; Hwang, K.G. Cell attachment and proliferation of osteoblast-like mg63 cells on silk fibroin membrane for guided bone regeneration. *Maxillofac. Plast. Reconstr. Surg.* **2016**, *38*, 17. [CrossRef] [PubMed]
26. Kim, S.G.; Kim, M.K.; Kweon, H.; Jo, Y.Y.; Lee, K.G.; Lee, J.K. Comparison of unprocessed silk cocoon and silk cocoon middle layer membranes for guided bone regeneration. *Maxillofac. Plast. Reconstr. Surg.* **2016**, *38*, 11. [CrossRef] [PubMed]
27. Ha, Y.Y.; Park, Y.W.; Kweon, H.; Jo, Y.Y.; Kim, S.G. Comparison of the physical properties and in vivo bioactivities of silkworm-cocoon-derived silk membrane, collagen membrane, and polytetrafluoroethylene membrane for guided bone regeneration. *Macromol. Res.* **2014**, *22*, 1018–1023. [CrossRef]
28. Kozubek, A.; Tyman, J.H. Resorcinolic lipids, the natural non-isoprenoid phenolic amphiphiles and their biological activity. *Chem. Rev.* **1999**, *99*, 1–26. [CrossRef] [PubMed]

29. Martı, O.; López-Caballero, M.; Montero, P.; Gómez-Guillén, M.D.C. Spraying of 4-hexylresorcinol based formulations to prevent enzymatic browning in norway lobsters (nephrops norvegicus) during chilled storage. *Food Chem.* **2007**, *100*, 147–155.
30. Rabbani, G.; Gilman, R.; Kabir, I.; Mondel, G. The treatment of fasciolopsis buski infection in children: A comparison of thiabendazole, mebendazole, levamisole, pyrantel pamoate, hexylresorcinol and tetrachloroethylene. *Trans. R. Soc. Trop. Med. Hyg.* **1985**, *79*, 513–515. [CrossRef]
31. Kang, Y.J.; Noh, J.E.; Lee, M.J.; Chae, W.S.; Lee, S.Y.; Kim, S.G. The effect of 4-hexylresorcinol on xenograft degradation in a rat calvarial defect model. *Maxillofac. Plast. Reconstr. Surg.* **2016**, *38*, 29. [CrossRef] [PubMed]
32. Park, Y.T.; Park, S.Y.; Kim, M.K.; Kim, S.G.; Park, Y.W.; Kwon, K.J. Effect of 4-hexylresorcinol on blood coagulation and healing of injured vessel in a rat model. *Maxillofac. Plast. Reconstr. Surg.* **2013**, *35*, 284–293. [CrossRef]
33. Kim, S.G.; JeonG, J.H.; Park, Y.W.; SonG, J.Y.; Kim, A.S.; CHoI, J.Y.; Chae, W.S. 4-hexylresorcinol inhibits transglutaminase-2 activity and has synergistic effects along with cisplatin in kb cells. *Oncol. Rep.* **2011**, *25*, 1597–1602. [CrossRef] [PubMed]
34. Kweon, H.; Kim, S.G.; Choi, J.Y. Inhibition of foreign body giant cell formation by 4-hexylresorcinol through suppression of diacylglycerol kinase delta gene expression. *Biomaterials* **2014**, *35*, 8576–8584. [CrossRef] [PubMed]
35. Panagiotopoulos, K.; Koutsouris, M.; Panagiotopoulos, E.; Antonopoulos, D.; Panagiotopoulos, V.; Papalois, A.; Kepenekidis, A. The effect of nifedipine on the patency of microvascular anastomosis in rats. *Acta. Chir. Plast.* **2008**, *50*, 33–35. [PubMed]
36. Lee, E.H.; Kim, J.Y.; Kweon, H.Y.; Jo, Y.Y.; Min, S.K.; Park, Y.W.; Choi, J.Y.; Kim, S.G. A combination graft of low-molecular-weight silk fibroin with choukroun platelet-rich fibrin for rabbit calvarial defect. *Oral Surg. Oral Med. Oral Pathol. Oral Radiol. Endod.* **2010**, *109*, e33–e38. [CrossRef] [PubMed]
37. Fukayama, T.; Takagi, K.; Tanaka, R.; Hatakeyama, Y.; Aytemiz, D.; Suzuki, Y.; Asakura, T. Biological reaction to small-diameter vascular grafts made of silk fibroin implanted in the abdominal aortae of rats. *Ann. Vasc. Surg.* **2015**, *29*, 341–352. [CrossRef] [PubMed]
38. Baguneid, M.; Seifalian, A.; Salacinski, H.; Murray, D.; Hamilton, G.; Walker, M. Tissue engineering of blood vessels. *Br. J. Surg.* **2006**, *93*, 282–290. [CrossRef] [PubMed]
39. Yu, E.; Mi, H.Y.; Zhang, J.; Thomson, J.A.; Turng, L.S. Development of biomimetic thermoplastic polyurethane/fibroin small-diameter vascular grafts via a novel electrospinning approach. *J. Biomed. Mater. Res. A* **2018**, *106*, 985–996. [CrossRef] [PubMed]
40. Liu, S.; Dong, C.; Lu, G.; Lu, Q.; Li, Z.; Kaplan, D.L.; Zhu, H. Bilayered vascular grafts based on silk proteins. *Acta Biomater.* **2013**, *9*, 8991–9003. [CrossRef] [PubMed]
41. Chantawong, P.; Tanaka, T.; Uemura, A.; Shimada, K.; Higuchi, A.; Tajiri, H.; Sakura, K.; Murakami, T.; Nakazawa, Y.; Tanaka, R. Silk fibroin-pellethane® cardiovascular patches: Effect of silk fibroin concentration on vascular remodeling in rat model. *J. Mater. Sci. Mater. Med.* **2017**, *28*, 191. [CrossRef] [PubMed]
42. Zhang, J.; Huang, H.; Ju, R.; Chen, K.; Li, S.; Wang, W.; Yan, Y. In vivo biocompatibility and hemocompatibility of a polytetrafluoroethylene small diameter vascular graft modified with sulfonated silk fibroin. *Am. J. Surg.* **2017**, *213*, 87–93. [CrossRef] [PubMed]
43. Yin, A.; Li, J.; Bowlin, G.L.; Li, D.; Rodriguez, I.A.; Wang, J.; Wu, T.; EI-Hamshary, H.A.; Al-Deyab, S.S.; Mo, X. Fabrication of cell penetration enhanced poly (l-lactic acid-co-ε-caprolactone)/silk vascular scaffolds utilizing air-impedance electrospinning. *Colloids Surf. B Biointerfaces* **2014**, *120*, 47–54. [CrossRef] [PubMed]
44. Zhu, M.; Wang, K.; Mei, J.; Li, C.; Zhang, J.; Zheng, W.; An, D.; Xiao, N.; Zhao, Q.; Kong, D. Fabrication of highly interconnected porous silk fibroin scaffolds for potential use as vascular grafts. *Acta Biomater.* **2014**, *10*, 2014–2023. [CrossRef] [PubMed]
45. Shimada, K.; Higuchi, A.; Kubo, R.; Murakami, T.; Nakazawa, Y.; Tanaka, R. The effect of a silk fibroin/polyurethane blend patch on rat vessels. *Organogenesis* **2017**, *13*, 115–124. [CrossRef] [PubMed]
46. Pérez-Rigueiro, J.; Elices, M.; Llorca, J.; Viney, C. Tensile properties of silkworm silk obtained by forced silking. *J. Appl. Polym. Sci.* **2001**, *82*, 1928–1935. [CrossRef]
47. Lamboni, L.; Gauthier, M.; Yang, G.; Wang, Q. Silk sericin: A versatile material for tissue engineering and drug delivery. *Biotechnol. Adv.* **2015**, *33*, 1855–1867. [CrossRef] [PubMed]

48. Harrison, G.J.; How, T.V.; Poole, R.J.; Brennan, J.A.; Naik, J.B.; Vallabhaneni, S.R.; Fisher, R.K. Closure technique after carotid endarterectomy influences local hemodynamics. *J. Vasc. Surg.* **2014**, *60*, 418–427. [CrossRef] [PubMed]
49. Byrne, J.; Feustel, P.; Darling, R.C., III. In Primary closure, routine patching, and eversion endarterectomy: What is the current state of the literature supporting use of these techniques? *Semin. Vasc. Surg.* **2007**, *20*, 226–235. [CrossRef] [PubMed]
50. Stone, P.A.; AbuRahma, A.F.; Mousa, A.Y.; Phang, D.; Hass, S.M.; Modak, A.; Dearing, D. Prospective randomized trial of acuseal versus vascu-guard patching in carotid endarterectomy. *Ann. Vasc. Surg.* **2014**, *28*, 1530–1538. [CrossRef] [PubMed]
51. Ostdiek, A.M.; Ivey, J.R.; Hansen, S.A.; Gopaldas, R.; Grant, S.A. Feasibility of a nanomaterial-tissue patch for vascular and cardiac reconstruction. *J. Biomed. Mater. Res. B Appl. Biomater.* **2016**, *104*, 449–457. [CrossRef] [PubMed]
52. Maertens, V.; Maertens, H.; Kint, M.; Coucke, C.; Blomme, Y. Complication rate after carotid endarterectomy comparing patch angioplasty and primary closure. *Ann. Vasc. Surg.* **2016**, *30*, 248–252. [CrossRef] [PubMed]
53. Anderson, J.M.; Rodriguez, A.; Chang, D.T. Foreign body reaction to biomaterials. *Semin. Immunol.* **2008**, *20*, 86–100. [CrossRef] [PubMed]
54. Anderson, J.M. Inflammatory response to implants. *ASAIO Trans.* **1988**, *34*, 101–107. [CrossRef] [PubMed]
55. Evans, R.; Baker, P.; Coburn, R.; Fischman, S.; Genco, R. In vitro antiplaque effects of antiseptic phenols. *J. Periodontol.* **1977**, *48*, 156–162. [CrossRef] [PubMed]
56. Ahn, J.; Kim, S.G.; Kim, M.K.; Kim, D.W.; Lee, J.H.; Seok, H.; Choi, J.Y. Topical delivery of 4-hexylresorcinol promotes wound healing via tumor necrosis factor-α suppression. *Burns* **2016**, *42*, 1534–1541. [CrossRef] [PubMed]
57. Kim, J.W.; Jo, Y.Y.; Kweon, H.Y.; Kim, D.W.; Kim, S.G. The effects of proteins released from silk mat layers on macrophages. *Maxillofac. Plast. Reconstr. Surg.* **2018**, *40*, 10. [CrossRef] [PubMed]
58. Fuster-Matanzo, A.; Manferrari, G.; Marchetti, B.; Pluchino, S. Wnt3a promotes pro-angiogenic features in macrophages in vitro: Implications for stroke pathology. *Exp. Biol. Med.* **2018**, *243*, 22–28. [CrossRef] [PubMed]
59. Katagiri, W.; Kawai, T.; Osugi, M.; Sugimura-Wakayama, Y.; Sakaguchi, K.; Kojima, T.; Kobayashi, T. Angiogenesis in newly regenerated bone by secretomes of human mesenchymal stem cells. *Maxillofac. Plast. Reconstr. Surg.* **2017**, *39*, 8. [CrossRef] [PubMed]
60. Cha, Y.H.; Nam, W.; Cha, I.H.; Kim, H.J. Revisiting radial forearm free flap for successful venous drainage. *Maxillofac. Plast. Reconstr. Surg.* **2017**, *39*, 14. [CrossRef] [PubMed]
61. Nelson, J.A.; Chung, C.U.; Bauder, A.R.; Wu, L.C. Prevention of thrombosis in hypercoagulable patients undergoing microsurgery: A novel anticoagulation protocol. *J. Plast. Reconstr. Aesthet. Surg.* **2017**, *70*, 307–312. [CrossRef] [PubMed]



© 2018 by the authors. Licensee MDPI, Basel, Switzerland. This article is an open access article distributed under the terms and conditions of the Creative Commons Attribution (CC BY) license (http://creativecommons.org/licenses/by/4.0/).